Forecasting and Impact Analysis of the Development Trends of China's New Energy Electric Vehicles Based on Time Series Causal Analysis

Qilian Ge [#], Enning Liu [#], Yingxin Qi [#, *]

Leicester International Institute, Dalian University of Technology, Dalian, China, 116024

* Corresponding Author Email: 18503603555@163.com

[#]These authors contributed equally.

Abstract. New energy electric vehicles with numerous properties have experienced explosive growth in recent years. This research constructs an ISM model to analyze the key factors influencing the new energy vehicle market and develops both a Winters' additive model and an ARIMA model to forecast the development of the NEV industry from 2023 to 2033. The results show that, the development of the new energy vehicles in the following ten years as a growth trend. Moreover, Granger causality tests, conducted within the VAR framework, revealed that NEV sales growth and market share significantly impact policy effectiveness and market dynamics. Simultaneously, the environmental impact was assessed using a LCA model, which indicates that the development of new energy vehicles is beneficial to the ecological environment. The results contribute to the theoretical and empirical understanding of the NEV market, providing valuable insights for policy makers and industry stakeholders.

Keywords: ISM Model, Time Series Model, VAR Model, Granger Causality Test, LCA Model.

1. Introduction

New energy electric vehicles, as a type of new energy vehicle with numerous properties such as superior power performance and environmental protection performance, having experienced explosive growth among consumers around the world in recent years. The new energy electric vehicle industry has also achieved tremendous development since the Chinese government formulated policies for the development of new energy electric vehicles. We will analyze the primary factors influencing the development of new NEV in China by ISM model and establish the time series model to forecast the development of the NEV industry in China over the next ten years. Next, conduct a temporal grant causality test to analyze the impact of new energy electric vehicles on the global traditional energy vehicle industry. Furthermore, perform a Robustness test and analysis the impact of the resistance policies on the development of new energy electric vehicles in China. Following, establish the LCA model to evaluate the impact on the ecological environment.

The research not only offers new insights into the critical driving factors of China's NEV market but also provides substantial empirical support for the future prospects of NEVs. Moreover, the study highlights the positive environmental impact of NEVs, providing significant reference for sustainable development policies.

2. Method

2.1. Winters' additive Model

The winters' additive Model is suitable for data that contains linear trends and stable seasonal components. The underlying principle and formula for this model are as follows [1-2].

$$\begin{cases} l_t = \alpha(\chi_t - s_{t-n}) + 11 - \alpha(l_{t-1} + b_{t-1}) \\ b_t = \beta(l_t - l_{t-1}) + (1-\beta)b_{t-1} \\ s_t = \gamma(x_t - l_{t-1} - b_{t-1}) + (1-\gamma)s_{t-m} \\ x_{t+h} = l_t + hb_t + s_{t+h-m(k+1)}, k = \left[\frac{h-1}{m}\right] \end{cases} \quad (1)$$

Compared to simple exponential smoothing, the winter's additive model incorporates a trend parameter, comprising both the level and trend components of forecasting, enabling adaptation to changes through bidirectional trend adjustments. However, a potential risk is its delayed response to significant numerical fluctuations caused by exogenous variables [2].

2.2. ARIMA Model

The basic principles of the ARIMA model can be expressed with the following formulas.

$$ARIMA(p,d,q) = AR(p) + I(d) + MA(q) \quad (2)$$

Where AR (p) denotes the autoregressive model, I (d) signifies the differencing model and MA (q) represents the moving average model.

The non-seasonal ARIMA model's differenced series is expressed.

$$y_t = \alpha_0 + \sum_{i=1}^{p} \alpha_i y_{t-i} + \varepsilon_t + \sum_{i=1}^{q} \beta_i \varepsilon_{t-i} \quad (3)$$

According to the autoregressive integrated moving average model, the seasonal ARIMA model extends the basic framework by incorporating seasonal terms.

$$(1 - \sum_{i-1}^{p} \alpha_i L^i)(1-L)^d y_t = \alpha_0 + (1 + \sum_{i=1}^{q} \beta_i L^i)\varepsilon_t \quad (4)$$

It succinctly represents the lag operator and specifies the parameters of the ARIMA model. ARIMA is employed to fit time series data, estimate appropriate model parameters, and facilitate forecasting and modeling. The algorithm aims to encapsulate the autoregressive nature of data, merging the strengths of differencing, autoregressive, and moving average models [3]. The model's prediction intervals are predicated on the assumption that residuals are uncorrelated and normally distributed, often necessitating autocorrelation tests on residuals prior to forecasting.

2.3. The VAR Model

The VAR model conducts linear regressions of all current variables on several lags of all variables, frequently utilized to analyze dynamic interrelationships among variables. This study focuses on the second-order VAR model, specifying the lag order of rt as described below [4-5].

$$\begin{cases} r_{1t} = \phi_{10} + \phi_{11} r_{1,t-1} + \phi_{12} r_{2,t-2} + \cdots + \phi_{1k} r_{k,t-k} + a_{1t} \\ r_{2t} = \phi_{20} + \phi_{21} r_{1,t-1} + \phi_{22} r_{2,t-2} + \cdots + \phi_{2k} r_{k,t-k} + a_{2t} \end{cases} \quad (5)$$

2.4. Temporal Granger Causality Test

The Granger causality test is a critical hypothesis test for coefficients within the VAR model. Assuming that in the aforementioned second-order VAR model, two series are coupled and the real-world model can be simplified to some certain coefficients, representing Granger causality being zero, the results of the VAR model can be further clarified by Granger causality test.

Consider a bivariate sequence $r_t = (r_{1t}, r_{2t})^T$. Let F_t represent the information available up to time t, and $F_{-i,t}$ denote the set of information in F_t excluding the i-th component. Consider a l-step ahead forecast based on F_t. Make predictions for $r_{2,t+l}$ using all available information up to time t, if

$$Ee_{2t}^2(l) = Var(r_{2,t+l} \mid F_t) < E\tilde{e}_{2t}^2(l) = Var(r_{2,t+l} \mid F_{-1,t}) \tag{6}$$

Which is a mean squared error smaller than that obtained without using the first component sequence, then r_{1t} is identified as a Granger cause of r_{2t}, implying that information from r_{1t} enhances the predictive accuracy of r_{2t} [4-6].

Utilizing VAR and VECM methodologies, causality among time series is examined by first constructing a model incorporating causal relationships, followed by testing the significance of parameters indicative of causality. Considering two time series, $\{X_t\}$ and $\{Y_t\}$, where $\{(X_t,Y_t)\}$ adheres to either weak or strict stationarity. If

$$\sigma^2(Y_t \mid \bar{Y}_t, \bar{X}_t) < \sigma^2(Y_t \mid \bar{Y}_t) \tag{7}$$

Then $\{X_t\}$ is deemed a Granger cause of $\{Y_t\}$, denoted as $X_t \Rightarrow Y_t$. If $X_t \Rightarrow Y_t$ holds, then the smallest positive integer m exists such that

$$\sigma^2(Y_t \mid \bar{Y}_t, X_{t-m}, X_{t-m-1}, \cdots) < \sigma^2(Y_t \mid \bar{Y}_t, X_{t-m-1}, X2, \cdots) \tag{8}$$

With m referred to as the causality lag [7]. If m exceeds 1, it implies that augmenting X_{t-1}, ⋯, X_{t-m+1} does not enhance the prediction of Y_t given Y_{t-1}, Y_{t-2}, ⋯ and X_{t-m}, X_{t-m-1}, ⋯ .

The limitation of employing VAR-based methods to test Granger causality is that all components must be stationary, precluding the use of counteraction models.

3. Experiments

3.1. Multi-layer hierarchical structure analysis based on ISM

Interpretive Structural Modeling (ISM) is a hierarchical analysis method designed for categorizing complex systems. It establishes and analyzes the relationships and influence pathways among elements within a multilevel system, decomposing the system into multiple subsystems and transforming it into a multistage hierarchical structure mode [8].

To construct an ISM model, initially establish the adjacency matrix A by enumerating the elements of the system and describing the existing relationships. Subsequently, compute the reachability matrix R. According to Boolean algebra, R is defined as the reachable matrix, satisfying the given expression.

$$(A+I)^{(n-1)} \neq (A+I)^n = (A+I)^{(n+1)} = R \tag{9}$$

Identify the reachability set R (Fi), the antecedent set Q (Fi), and their intersection C (Fi), the reachability matrix is then iteratively decomposed into layer. When C (Fi) = R (Fi) identifies Fi as the top-tier factor, it is positioned at the first level of the ISM model. This method is repeated to discern secondary and tertiary factors until all elements are stratified.

Table 1. The process of hierarchical iterative.

Factor	Reachable Set (F_i)	Antecedent Set (Q_i)	Common Set (C_i)
F_1	$F_1, F_2, F_3, F_5, F_6, F_7, F_8, F_9, F_{10}, F_{12}$	F_1	F_1
F_2	$F_2, F_5, F_6, F_7, F_8, F_9, F_{10}, F_{12}$	F_1, F_2	F_2
F_3	$F_3, F_5, F_6, F_7, F_8, F_9, F_{10}, F_{12}$	F_1, F_3	F_3
F_4	F_4, F_{10}	F_4	F_4
F_5	$F_5, F_6, F_7, F_8, F_9, F_{10}, F_{12}$	F_1, F_2, F_3, F_5, F_7	F_5, F_7
F_6	$F_6, F_8, F_9, F_{10}, F_{12}$	$F_1, F_2, F_3, F_5, F_6, F_7$	F_6
F_7	$F_5, F_6, F_7, F_8, F_9, F_{10}, F_{12}$	F_1, F_2, F_3, F_5, F_7	F_5, F_7
F_8	F_8, F_9, F_{10}, F_{12}	$F_1, F_2, F_3, F_5, F_6, F_7, F_8, F_9$	F_8, F_9
F_9	F_8, F_9, F_{10}, F_{12}	$F_1, F_2, F_3, F_5, F_6, F_7, F_8, F_9$	F_8, F_9
F_{10}	F_{10}, F_{11}	$F_1, F_2, F_3, F_4, F_5, F_6, F_7, F_8, F_9, F_{10}, F_{11}$	F_{10}, F_{11}
F_{11}	F_{10}, F_{11}	F_{11}	F_{11}
F_{12}	F_{12}	$F_1, F_2, F_3, F_5, F_6, F_7, F_8, F_9, F_{12}$	F_{12}

From Table 1, we can visualize the hierarchical iterative process.

Based on the hierarchical levels derived from interval decomposition, reorganize the reachability matrix, eliminating reflexive and transitive relations between layers to ultimately derive the structured matrix R.

3.2. LCA model

The Life Cycle Assessment (LCA) model provides an objective evaluation of the environmental burden associated with a product, process, or specific behavior, encompassing impacts from production to disposal. It quantifies these impacts using the equation below.

$$T=P+U+W \tag{10}$$

T represents the total environmental impact, *P* denotes the impact during the production stage, *and U* is the impact during the usage stage and *W* is the impact at the waste stage. The lifecycle of a new energy vehicle is bifurcated into two components, which are the vehicle cycle and the fuel cycle.

3.2.1. The production stage of the vehicle

The production stage of the vehicle is primarily segmented into three components: the vehicle body, the power battery, and fluids. These, combined with gasoline consumption, electricity consumption, and repair and replacement, culminate in six environmental impacts that collectively form the vehicle cycle [9].

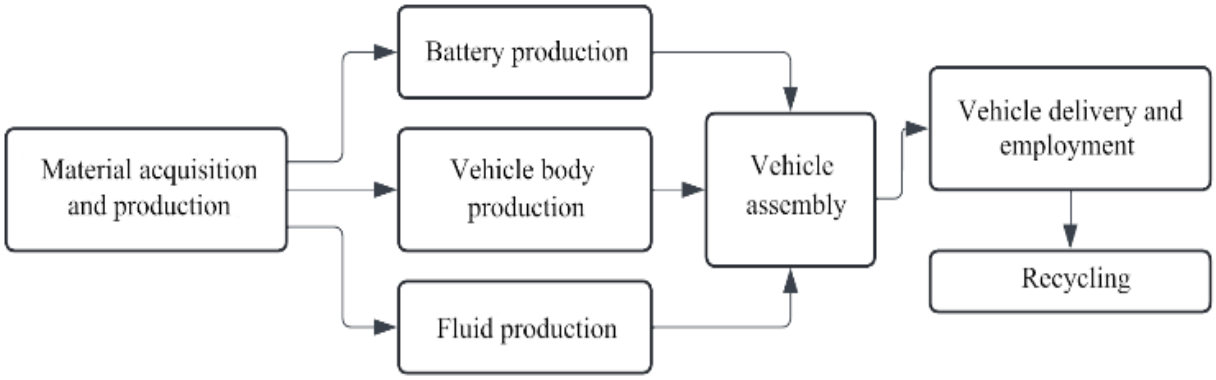


Figure 1. The production stage of the vehicle.

The production stage of the vehicle is demonstrated in Figure 1 and it also shows the six environmental impacts.

Environmental impact of vehicle main body production can be calculated as follows.

$$E_{V1,i}=\sum_{j}(M_{V1,j}\times f_{j,i}) \tag{11}$$

Environmental impact of vehicle battery production can be calculated as follows.

$$E_{V2,i}=E_{Bs,i}+E_{Ps,i} \tag{12}$$

The environmental impact of the fluid production process is calculated as follows.

$$E_{V3,i}=\sum_{l}E_{l,i} \tag{13}$$

3.2.2. The fuel production process

The fuel production process is considered as the upstream phase of the fuel cycle (WTP), while the use of the fuel is consumed as the downstream phase of the fuel cycle (PTW).

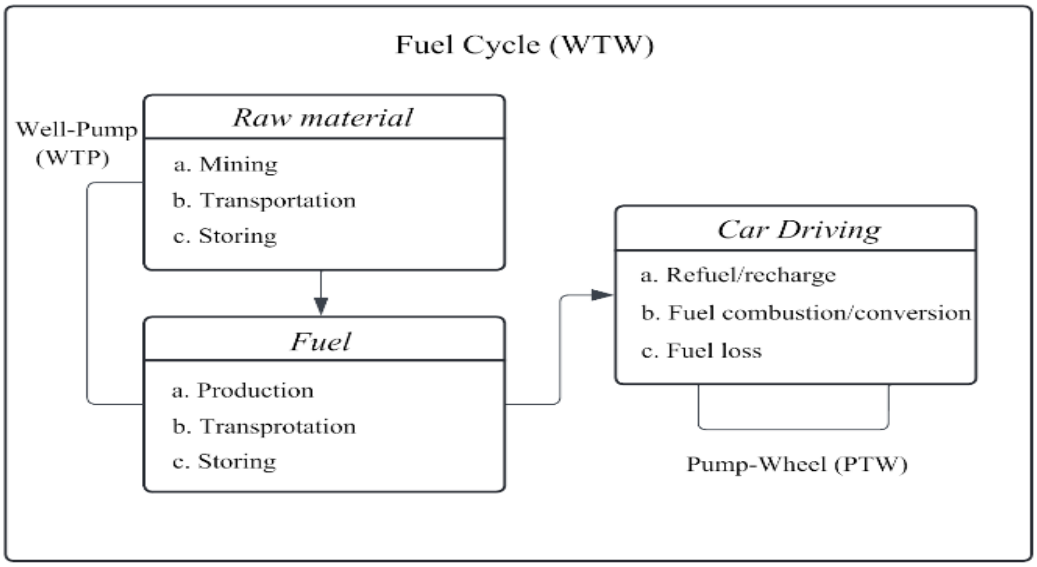


Figure 2. The fuel production process.

Figure 2 demonstrates the fuel production process, which contains the Well-Pump and Pumpp-Wheel stage.

Energy consumption in the WTP stage is related to the conversion efficiency of fuel in PTW stage η and fuel consumption in production, processing and transportation $E_{i,j,k}$ [10].

The WTP stage is mainly the fuel consumption of the vehicle, and each energy consumption is closely related to the fuel economy of the vehicle (Fuel Economy).

$$E_{WTP_j} = \frac{E_{PTW_j}}{\eta} - E_{PTW_j} + \sum_i \sum_k E_{j,i,k} \tag{14}$$

The PTW stage is mainly the fuel consumption of the vehicle, and each energy consumption is closely related to the fuel economy of the vehicle (Fuel Economy).

$$E_{PTW_j} = LHV_j \times \rho_j \times FE_j \div 100 \tag{15}$$

3.2.3. Environmental impact potential assessment

Environmental impact assessment have the following five criteria [10-12]:

(1)Energy consumption EU

$$EU = E_{up} + E_{\text{use}} \tag{16}$$

(2)Global warming potential GWP

$$GWP = \sum_i GWP_i \cdot m_i \tag{17}$$

(3)Acidification potential AP

$$AP = \sum_i AP_i \cdot m_i \tag{18}$$

(4)Inhalable particulate matter RI

$$RI = \sum_i M_{PM10} \tag{19}$$

(5)Human biological toxicity potential HTP

$$HTP = \sum_i HTP_i \cdot m_i \tag{20}$$

4. Results

4.1. The Analysis of the influencing factors by ISM model

This study employs the Porter diamond model, synthesizing literature reviews and expert group discussions, to identify the principal factors influencing the development of new energy electric vehicles [9].

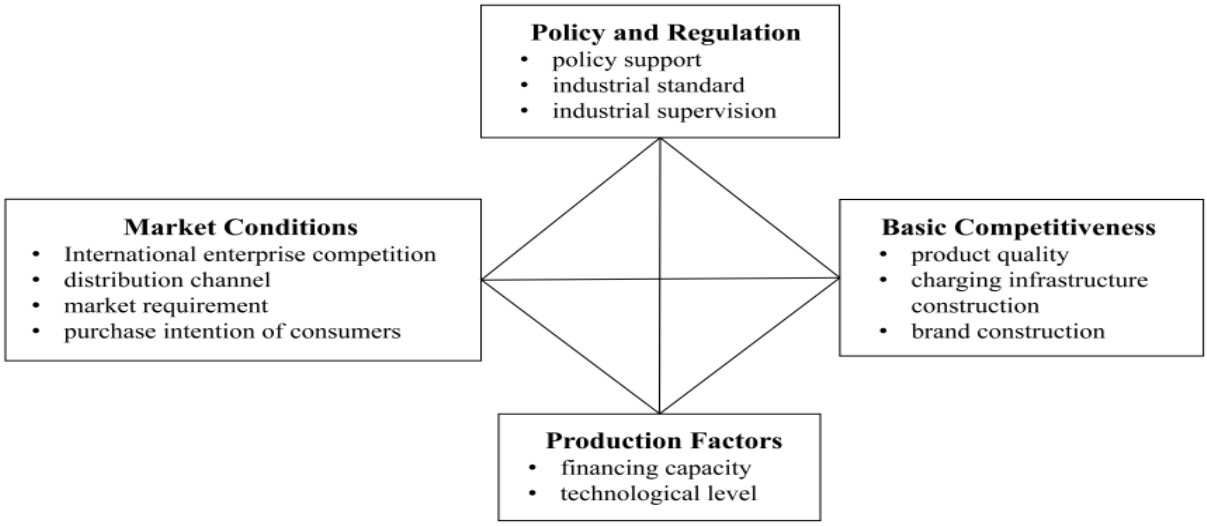


Figure 3. The diamond model of influencing factors.

These factors are categorized into four dimensions comprising 12 representative elements, as illustrated in Figure 3.

The development environment for new energy electric vehicles is systematized, encompassing 12 primary influencing factors denoted as F_i (i=1, 2, 3...12). An interpretive structural model of these factors reveals a six-tier hierarchical directed structure, visually articulated through a hierarchical diagram that outlines the interrelationships among these factors, as depicted in Figure 4.

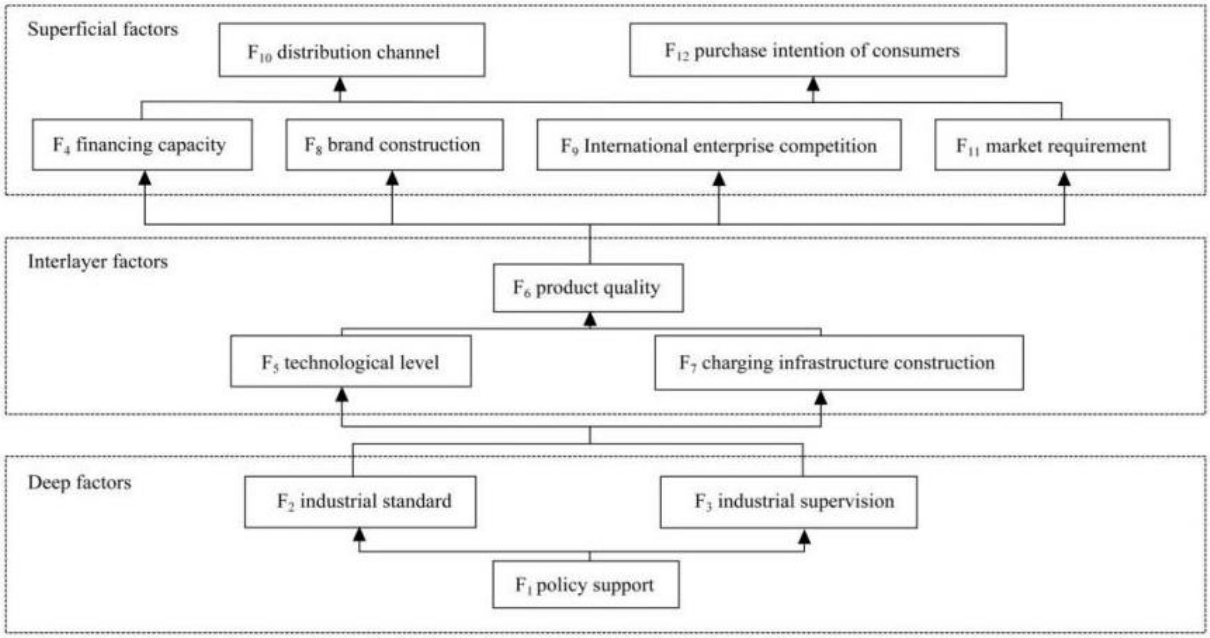


Figure 4. Hierarchical structure diagram.

4.2. Sales Forecasting

4.2.1. Quarterly Forecast

Sales data for new energy vehicles in China was collected from Q1 2016 to Q3 2023 with no missing values. Using SPSS, a time series plot was created and analyzed, revealing an overall upward trend with seasonal fluctuations during the observation period.

Table 2. Modeling Statistics.

Model	Number of predictors	Model fit degree statistics R-squared value	Liung-BOX Q (18) Satistics	DF	Significance
Sales volume (ten thousand)	0	.308	19.002	15	.214

From Table 2, time series decomposition via SPSS Expert Modeler showed no significant differences in the residual ACF plot with a Q-test p-value of 0.214, indicating the winter's additive model effectively captures the sales data pattern.

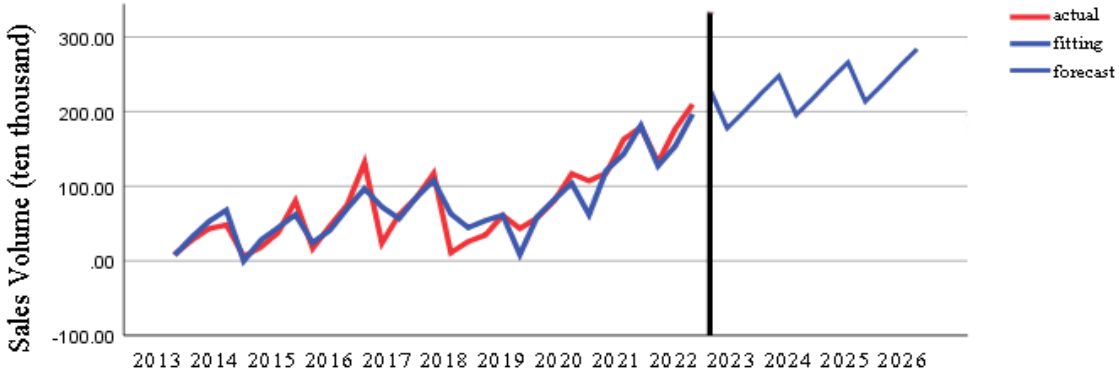


Figure 5. Prediction Results of Quarterly.

Figure 5 shows the prediction results of quarterly. The forecast results demonstrate a good fit between the model and the original data, preserving seasonal effects and showing an upward linear trend in sales predictions for the next four years.

4.2.2. Annual Sales Forecast

The data was differenced and an ARIMA (0, 1, and 0) model was identified.

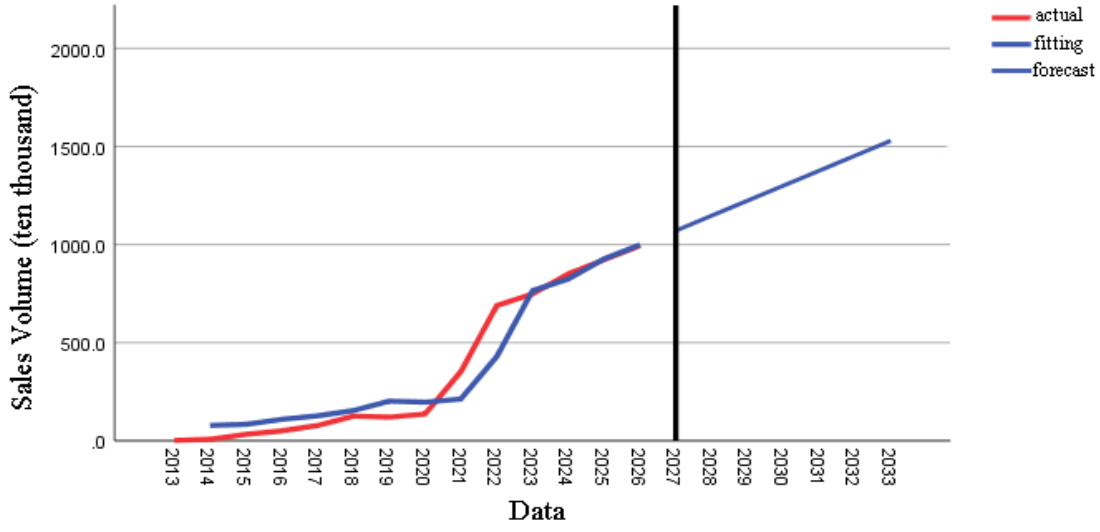


Figure 6. Prediction Results of Annual.

In Figure 6, both the residual ACF and PACF plots showed no significant discrepancies, the fitted model's R2 value was 0.937.

Table 3. Sales volume with years.

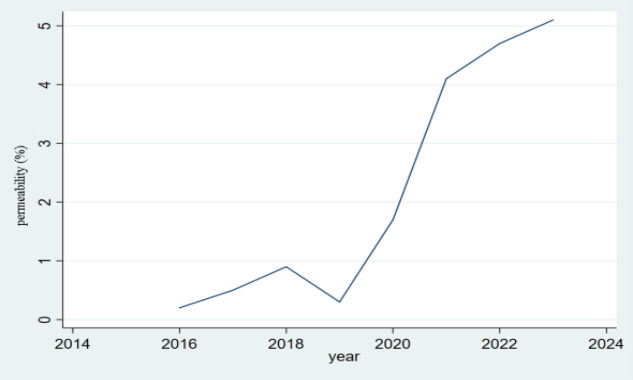
YEAR	Sales Volume (ten thousand)
2023	748.3
2024	851.0
2025	922.8
2026	994.7
2027	1071.1
2028	1147.5
2029	1223.8
2030	1300.2
2031	1376.6
2032	1453.0
2033	1529.3

Considering the overall upward sales trend, this model provides well-fitted and reliable forecasts of total new energy vehicle sales in mainland China for the next decade. The sales volume with years from year 2023 to year 2033 is listed in Table 3.

4.3. Impact Analysis

4.3.1. Annual Sales Forecast

The core metric for examining the issue is market penetration. Subsequently, time series data on sales and sales growth rates for both the new energy vehicle industry and the traditional automotive industry are collected to establish a VAR model and perform a standard Granger causality test. Meanwhile, a second-order difference is implemented to ensure analytical accuracy.



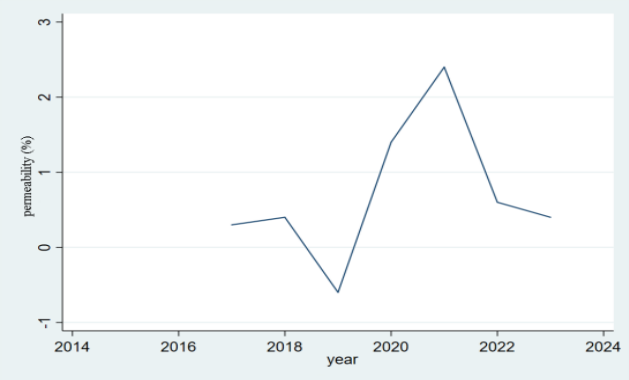


Figure 7. First-order difference of permeability. **Figure 8.** Second-order difference of permeability.

The first-order and second-order difference of the penetration rate are obtained in figure 7 and figure 8.

Setting the significance level at 0.05, it can be concluded that sales growth, NEV sales and NEV share are Granger causes of the policy effect.

Table 4. Results of the Temporal Granger Causality Test.

Dependent Variable of the Equation	Test Variable	P-Value for the Test Variable	Result
Electricity Demand	Sales Growth	0.0414	Sales growth is a Granger cause of electricity demand.
Policy Effect	Sales Growth	0.0416	Sales growth, NEV sales and NEV share are Granger causes of policy effect.
	NEV Sales	0.0464	
	NEV Share	0.0461	

From the results of the temporal Granger causality test of Table 4, we know that sale growth is a Granger cause of electricity demand. Meanwhile, sales growth, NEV sales and NEV share are Granger causes of policy effect.

The impact of China's new energy electric vehicle industry on the traditional automotive sector is not only reflected in the rapid expansion of market share, but in its positive influence on policy support and the development of more comprehensive charging infrastructure and power supply.

4.3.2. Impact on the Ecological Environment

The three most popular types of new energy vehicles, namely ICE, HEV and EV, were included in the study. According to the literature, the full life cycle impact of new energy charging piles encompasses private and public AC/DC/AC/DC integrated charging piles. The total life cycle energy consumption is 89,112 MJ, 158,890 MJ, 2,206,182 MJ, and 2,364,378 MJ, respectively [9]. The environmental potential assessment form is obtained by calculation.

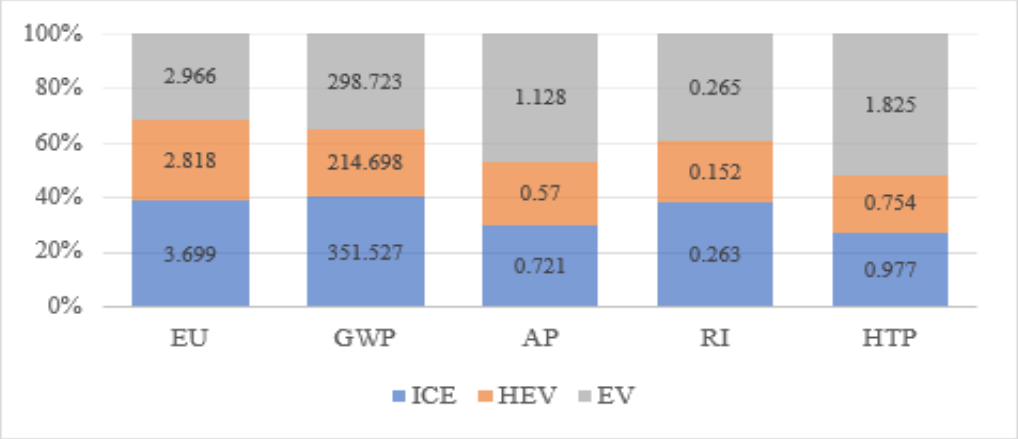


Figure 9. Environmental potential assessment form.

The environmental potential assessment form is shown in Figure 9.

According to the problem and model hypothesis, the electrification degree of new energy vehicles in the city at this stage reduces the total energy consumption by 5.97%.

5. Conclusions

This study analyzed China's new energy electric vehicle (NEV) industry using ISM, winters' additive model, ARIMA, VAR, and LCA models. The ARIMA model provided reliable annual sales forecasts, demonstrating a clear upward trend in NEV adoption. Granger causality tests, conducted within the VAR framework, revealed that NEV sales growth and market share significantly impact policy effectiveness and market dynamics. The ISM model identified and hierarchically structured 12 key factors influencing the NEV market, offering insights for stakeholders. The LCA model assessed environmental impacts, indicating substantial energy consumption across different charging infrastructures but also potential reductions in total energy use and environmental burdens with increased NEV adoption. The expansion of China's NEV market drives policy innovation and infrastructure development while yielding environmental benefits, underscoring the importance of sustainable vehicle technologies. Future research should refine predictive models and examine the long-term ecological impacts of NEV adoption.

References

[1] Şahinli M A. Potato price forecasting with Holt-Winters and ARIMA methods: A case study [J]. American Journal of Potato Research, 2020, 97(4): 336-346.

[2] Hansun S, Charles V, Indrati C R. Revisiting the Holt-Winters' additive method for better forecasting [J]. International Journal of Enterprise Information Systems (IJEIS), 2019, 15(2): 43-57.

[3] Sahai A K, Rath N, Sood V, et al. ARIMA modelling & forecasting of COVID-19 in top five affected countries [J]. Diabetes & metabolic syndrome: clinical research & reviews, 2020, 14(5): 1419-1427.

[4] Hamilton J D. Time series analysis [M]. Princeton university press, 2020.

[5] Kumar R, Kumar P, Kumar Y. Multi-step time series analysis and forecasting strategy using ARIMA and evolutionary algorithms [J]. International Journal of Information Technology, 2022, 14(1): 359-373.

[6] Shojaie A, Fox E B. Granger causality: A review and recent advances [J]. Annual Review of Statistics and Its Application, 2022, 9(1): 289-319.

[7] Amornbunchornvej C, Zheleva E, Berger-Wolf T Y. Variable-lag granger causality for time series analysis[C]//2019 IEEE International Conference on Data Science and Advanced Analytics (DSAA). IEEE, 2019: 21-30.

[8] Anthony Bagherian, Analyzing the relationship between digitalization and energy sustainability: A comprehensive ISM-MICMAC and DEMATEL approach [J], Expert Systems with Applications, 2024, Volume 236.

[9] Weike Zhang, Does de-capacity policy enhance the total factor productivity of China's coal companies? A Regression Discontinuity design [J], Resources Policy, 2020, Volume 68.

[10] Zhang B, Lu Q, Wu P. Study on life-cycle energy impact of new energy vehicle car-sharing with large-scale application [J]. Journal of Energy Storage, 2021, 36: 102334.

[11] Yu R, Cong L, Hui Y, et al. Life cycle CO2 emissions for the new energy vehicles in China drawing on the reshaped survival pattern[J]. Science of the Total Environment, 2022, 826: 154102.

[12] Li L, Yue C, Ma S, et al. Life cycle assessment of car energy transformation: evidence from China [J]. Annals of Operations Research, 2023: 1-20.